J|A|C|S
ARTICLES

Published on Web 04/15/2009

Fluorescent BODIPY-Based Zn(II) Complex as a Molecular Probe for Selective Detection of Neurofibrillary Tangles in the Brains of Alzheimer's Disease Patients

Akio Ojida,[†,‡] Takashi Sakamoto,[†] Masa-aki Inoue,[†] Sho-hei Fujishima,[†] Guy Lippens,[§] and Itaru Hamachi*[,†,||]

Department of Synthetic Chemistry and Biological Chemistry, Graduate School of Engineering, Kyoto University, Katsura campus, Kyoto 615-8510, Japan, JST, PRESTO (Life Phenomena and Measurement Analysis), Sanbancho, Chiyodaku, Tokyo 102-0075, Japan, CNRS-Université de Lille 1, UMR 8576, USTL, Avenue de Mandeleiev, 59655 Villeneuve d'Ascq Cedex, France, and JST, CREST (Creation of Next-generation Nanosystems through Process Integration), Sanbancho, Chiyodaku, Tokyo 102-0075, Japan

Received February 4, 2009; E-mail: ihamachi@sbchem.kyoto-u.ac.jp

Abstract: We have developed a new fluorescent binuclear Zn(II) complex for the detection of neurofibrillary tangles (NFTs) of hyperphosphorylated tau proteins, a representative hallmark of Alzheimer's disease (AD). The probe **1** incorporates a fluorescent BODIPY unit and two Zn(II)−2,2′-dipicolylamine (Dpa) complexes as a binding site for phosphorylated amino acid residues. Using fluorescence titration to evaluate the binding and sensing properties of **1** toward several phosphorylated peptide segments derived from hyperphosphorylated tau protein, we found that **1** binds preferentially to peptides presenting phosphorylated groups at the *i* and *i*+4 positions with dissociation constants (K_d) in the micromolar range. Fluorescence titration with an artificially prepared aggregate of the phosphorylated tau protein (p-Tau) revealed that **1** binds strongly to p-Tau ($EC_{50} = 9$ nM). In contrast, the interactions of **1** were weaker toward artificially prepared aggregates of the nonphosphorylated tau protein (n-Tau; $EC_{50} = 80$ nM) and Aβ_{1-42} fibrils ($EC_{50} = 650$ nM). Histological imaging of a hippocampus tissue section obtained from an AD patient revealed that **1** fluorescently visualizes deposits of NFTs and clearly discriminates between NFTs and the amyloid plaques assembled from amyloid-β peptides, confirming our strategy toward the rational design of a molecular probe for the selective fluorescence detection of NFTs in brain tissue sections.

Introduction

Phosphorylation is a prevalent regulatory mechanism of many protein functions; it plays a central role in many biological processes.[1] Protein phosphorylation is usually controlled in terms of the number of phosphate units and their position through the individual action of protein kinases and phosphatases. An overall imbalance of their activities can cause aberrant hyperphosphorylation of proteins, which sometimes leads to serious disruption of cellular functions.[2] A representative example is the hyperphosphorylation of tau proteins. Tau is a microtubule-associated protein that is present in high abundance in neuronal cells. The binding of tau to microtubules is primarily regulated by serine/threonine-directed phosphorylations. Under pathological conditions, however, tau is abnormally hyperphosphorylated at more than 30 sites and, as a result, loses its binding ability to microtubles.[3] The liberated hyperphosphorylated tau accumulates in brain tissue as insoluble filamentous aggregates, so-called neurofibrillary tangles (NFTs).[4] It is widely recognized that insoluble deposits of NFTs and the senile plaques (SPs) assembled from β-amyloid peptide (Aβ) are the representative pathological hallmarks of many neurodegenerative disorders, including Alzheimer's disease (AD).[5] In the past two decades, many studies have been devoted to understanding of the deleterious effects of NFTs and SPs in the progress of dementia; nevertheless, the mechanistic linkages between these two fibrillar formations and their functional relationships in various neurodegenerative diseases remain controversial.[6] The development of a functional molecular probe that enables the individual

† Kyoto University.
‡ JST, PRESTO.
§ CNRS-Université de Lille 1.
|| JST, CREST.

(1) (a) Hunter, T. *Protein Phosphorylation*; Academic Press: New York, 1998. (b) Pawson, T.; Scott, J. D. *Trends Biochem. Sci.* **2005**, *30*, 286–290.
(2) (a) Götz, J.; Ittner, L. M. *Nat. Rev. Neurosci.* **2008**, *9*, 532–544. (b) Chakraborti, S.; Das, S.; Kar, P.; Ghosh, B.; Samanta, K.; Kolley, S.; Ghosh, S.; Roy, S.; Chakraborti, T. *Mol. Cell. Biochem.* **2007**, *298*, 1–40. (c) Veeramani, S.; Yuan, T. C.; Chen, S. J.; Lin, F. F.; Petersen, J. E.; Shaheduzzaman, S.; Srivastava, S.; MacDonald, R. G.; Lin, M. F. *Endocr. Relat. Cancer* **2005**, *12*, 805–822.
(3) (a) Hanger, D. P.; Byers, H. L.; Wray, S.; Leung, K. Y.; Saxton, M. J.; Seereeram, A.; Reynolds, C. H.; Ward, M. A.; Anderton, B. H. *J. Biol. Chem.* **2007**, *282*, 23645–23654. (b) Lindwall, G.; Cole, R. D. *J. Biol. Chem.* **1984**, *259*, 5301–5305.
(4) Lee, V. M.; Balin, B. J.; Otvos, L., Jr.; Trojanowski, J. Q. *Science* **1991**, *251*, 675–678.
(5) Goedert, M.; Spillantini, M. G. *Science* **2001**, *314*, 777–781.
(6) (a) King, M. E.; Kan, H. M.; Baas, P. W.; Erisir, A.; Glabe, C. G.; Bloom, G. S. *J. Cell. Biol.* **2006**, *175*, 541–546. (b) Leschik, J.; Welzel, A.; Weissmann, C.; Eckert, A.; Brandt, R. *J. Neurochem.* **2007**, *101*, 1303–1315. (c) Rapoport, M.; Dawson, H. N.; Binder, L. I.; Vitek, M. P.; Ferreira, A. *Proc. Natl. Acad. Sci. U.S.A.* **2002**, *99*, 6364–6369.

detection of NFTs and SPs would benefit approaches based on fluorescence imaging or positron emission tomography (PET) to allow a more precise understanding of the pathophysiology of neurodegenerative diseases. For this purpose, several small molecular probes have been developed,[7] but none of them has been able to discriminate between NFTs and SPs with high specificity.[8]

In this Article, we report the rational design, function, and application of the binuclear Zn(II) complex **1** as a fluorescent probe for the selective detection of NFTs in brain tissue. The strong binding of **1** toward aggregated hyperphosphorylated tau proteins enables a simple staining procedure to be used for the selective fluorescence imaging of NFTs. Notably, a sharp discrimination of NFTs from SPs results from the phospho-selective binding properties of **1**, based on multivalent metal−ligand interactions with multiple phosphorylated sites of the tau protein.

Experimental Section

Fluorescence Titration of Tau Peptide With Probe 1. Fluorescence spectra were recorded on a Perkin−Elmer LS55 spectrofluorophotometer. The fluorescence quantum yield of **1** was determined in neutral aqueous solution (50 mM HEPES, pH 7.2) using rhodamine B (Sigma, SL, US) as a standard ($\Phi = 0.31$).[9] The titration experiments with the phosphorylated peptides were performed at 25 °C using a solution of **1** (5 μM) or **3** (5 μM) in 50 mM HEPES (pH 7.2, 3 mL) in a quartz cell. The fluorescence emission spectra (excitation wavelength; $\lambda_{ex} = 480$ nm) were measured after addition (via a micro syringe) of a freshly prepared aqueous solution of the peptide. Fluorescence titration curves ($\lambda_{em} = 545$ nm) were analyzed using nonlinear least-squares curve-fitting to evaluate the dissociation constant (K_d).

Preparation of Phosphorylated Tau (p-Tau) Protein. The N-terminus 6His-tagged full-length tau protein (n-Tau, 447 amino acids) was expressed in Tau441-pET15b-transformed *Escherichia coli* BL21(DE3) and purified through a HisTag affinity column according to the reported procedure.[10] The purified n-Tau protein (200 μg/mL, 4.4 μM) was phosphorylated through treatment with GSK-3β (4.6 units/pmol of Tau protein, New England Biolabs) in 40 mM HEPES (pH 7.6; containing 5 mM EGTA, 3 mM $MgCl_2$, and 2 mM ATP) for 24 h at 30 °C. The buffer was exchanged to HBS buffer through dialysis at 4 °C (MWCO = 3500). The concentration of the phosphorylated tau protein (p-Tau) was determined using the BCA method with BSA as a standard. The average phosphorylation number of p-Tau was determined through in-gel fluorescence analysis using ProQ diamond (Invitrogen) as a staining reagent; ovalbumin (2 mol of phosphate/mol of protein) was used as a standard phosphorylated protein.

Preparation of in Vitro Aggregates. Aggregates of the p-Tau and n-Tau proteins were prepared according to the reported method.[11] Briefly, the purified p-Tau or n-Tau protein (8 μM) was incubated with heparin (1.6 μM) in 10 mM HEPES buffer (pH 7.6) containing 40 mM NaCl, 0.1 mM EDTA, and 5 mM DTT at 37 °C for 1−20 days. The formation of the aggregates was confirmed using transmitted electron microscopy (TEM) and fluorescence titration with thioflavin-T. The Aβ_{1-42} fibril was prepared according to a reported method.[12] Briefly, an aqueous ammonium hydroxide solution (0.02%) of Aβ_{1-42} peptide (250 μM, Wako Pure Chemical) was diluted 10-fold with HBS and left to stand for 3 days at 37 °C.

Fluorescence Titration of in Vitro Aggregates With Probe 1. A suspension of p-Tau (8 μM) or Aβ_{1-42} aggregate (25 μM) was sequentially diluted (1:25 to 1:6500 for p-Tau; 1:2.5 to 1:320 for Aβ) with HBS buffer [containing 10% (v/v) DMSO and 10 μM $Zn(NO_3)_2$], and then each diluted solution was mixed with a solution of **1** (100 nM) in HBS buffer. After incubation for 2.5 h at 37 °C, the fluorescence intensity (545 nm) of each solution was measured using a fluorescence microplate reader (Infinite M200, TECAN) with excitation at 490 nm.

Evaluation of the EC_{50} of 1 for the in Vitro Aggregates. A suspension of the aggregate (1 μg/mL) of p-Tau, n-Tau, or Aβ_{1-42} was incubated with 0.3 nM−3.3 μM of **1** in HBS [containing 10% (v/v) DMSO and 100 μM $Zn(NO_3)_2$] at 37 °C for 10 min. The fluorescence intensity (545 nm) of each solution was measured using a microplate reader (Infinite M200, TECAN) with excitation at 490 nm. The EC_{50} values (defined as the effective concentration of **1** required to achieve 50% of the maximal fluorescence change) were calculated using IgorPro software (WaveMetrics, Inc.).

Fluorescence Staining of in Vitro Aggregates. A suspension of p-Tau, n-Tau, or Aβ_{1-42} aggregate was diluted 4-fold with an HBS buffer solution of **1** (10 μM) and thioflavin T (10 μM), and then the mixture was incubated for 10 min at room temperature. For the control experiment, sodium pyrophosphate (PPi, 100 μM) was added to the solution. After centrifugation (15 000 rpm, 15 min, 4 °C), the supernatant was discarded, and the collected aggregate was washed twice with 0.5 mM aqueous $Zn(NO_3)_2$. The aggregate was resuspended in 0.5 mM aqueous $Zn(NO_3)_2$ (10 μL), and then a portion of this suspension (0.5 μL) was placed onto a glass slip (22 × 24 mm; thickness: 0.12−0.17 mm) and air-dried. The fluorescence images were obtained through confocal laser scanning microscopy (FV-1000, Olympus) using an optimal excitation laser and detection wavelength window for each fluorescent dye (probe **1**, $\lambda_{ex} = 488$ nm, $\lambda_{em} = 560-580$ nm; thioflavin T, $\lambda_{ex} = 458$ nm, $\lambda_{em} = 470-490$ nm).

Fluorescence Immunohistochemical Staining of Brain Tissue Sections. Paraffin-embedded human hippocampus tissue sections from an Alzheimer's disease patient and a healthy adult were purchased from BioChain Institute (CA). The tissue sections were deparaffinized using a standard procedure employing xylene and ethanol. To remove the fluorescent deposits of lipofuscin, the deparaffinized tissue section was incubated in 0.25 wt % $KMnO_4$/PBS for 30 min and then washed twice with PBS. The tissue section was incubated in PBS containing 1 wt % oxalic acid and 1 wt % potassium pyrisulfate for 6 min and then washed with PBS. The tissue section was treated with trypsin (0.05 wt % in PBS) for 15 min at 37 °C and then washed with PBS containing 0.2 wt % Tween 20 (PBS-Tween) to retrieve antigen activity. For the dephosphorylation of NFTs,[13] the tissue section was treated with trypsin and then incubated with PP2A (0.5 units, Upstate) for 24 h at 37 °C. After blocking with 10% goat serum in PBS for 1 h at 37 °C, a

(7) (a) Raymond, S. B.; Skoch, J.; Hills, I. D.; Nesterov, E. E.; Swager, T. M.; Bacskai, B. J. *Eur. J. Nucl. Med. Mol. Imaging* **2008**, *35*, S93−98. (b) Li, Q.; Min, J.; Ahn, Y. H.; Namm, J.; Kim, E. M.; Lui, R.; Kim, H. Y.; Ji, Y.; Wu, H.; Wisniewski, T.; Chang, Y. T. *ChemBioChem* **2007**, *8*, 1679–1687. (c) Nilsson, K. P.; Aslund, A.; Berg, I.; Nyström, S.; Konradsson, P.; Herland, A.; Inganäs, O.; Stabo-Eeg, F.; Lindgren, M.; Westermark, G. T.; Lannfelt, L.; Nilsson, L. N.; Hammarström, P. *ACS Chem. Biol.* **2007**, *2*, 553–560. (d) Shin, J.; Lee, S. Y.; Kim, S. H.; Kim, Y. B.; Cho, S. J. *Neuroimage* **2008**, *43*, 236–244. (e) Henriksen, G.; Yousefi, B. H.; Drzezga, A.; Wester, H. J. *Eur. J. Nucl. Med. Mol. Imaging* **2008**, *35*, S75−S81. (f) Nordberg, A. *Eur. J. Nucl. Med. Mol. Imaging* **2008**, *35*, S46−S50. (g) Nordberg, A. *Curr. Opin. Neurol.* **2007**, *20*, 398–402.
(8) Okamura, N.; Suemoto, T.; Furumoto, S.; Suzuki, M.; Shimadzu, H.; Akatsu, H.; Yamamoto, T.; Fujiwara, H.; Nemoto, M.; Maruyama, M.; Arai, H.; Yanai, K.; Sawada, T.; Kudo, Y. *J. Neurosci.* **2005**, *25*, 10857–10862.
(9) Magde, D.; Rogas, G. E.; Seybold, P. G. *Photochem. Photobiol.* **1999**, *70*, 737–744.
(10) Lippens, G.; Wieruszeski, J. M.; Leroy, A.; Smet, C.; Sillen, A.; Buée, L.; Landrieu, I. *ChemBioChem* **2004**, *5*, 73–78.
(11) Carlson, S. W.; Branden, M; Voss, K.; Sun, Q.; Rankin, C. A.; Gamblin, T. C. *Biochemistry* **2007**, *46*, 8838–8849.
(12) Murakami, K.; Irie, K.; Morimoto, A.; Ohigashi, H.; Shindo, M.; Nagao, M.; Shimizu, T.; Shirasawa, T. *Biochem. Biophys. Res. Commun.* **2002**, *294*, 5–10.
(13) Liu, F.; Grundke-Iqbal, I.; Iqbal, K.; Gong, C. X. *Eur. J. Neurosci.* **2005**, *22*, 1942–1950.

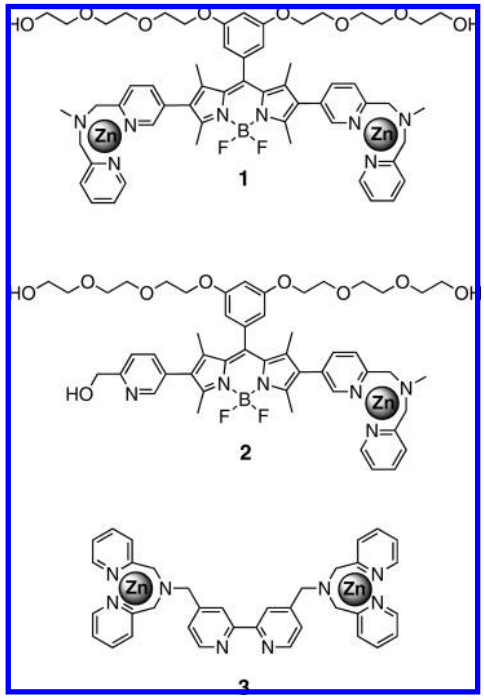

Figure 1. Structures of probes **1**−**3**.

solution of primary mouse monoclonal antibodies AT8 (1:5000, Innogenetics) or Tau2 (1:5000, Sigma) was poured onto the tissue section, which was then incubated overnight at 4 °C. After being washed with PBS-Tween on ice (5 × 2 min), the tissue section was incubated with antimouse IgG goat IgG (Invitrogen, 1:500) labeled with AlexaFluor 633 in 5% goat serum/PBS for 1 h at 37 °C, and then it was washed with PBS-Tween on ice (3 × 2 min). The tissue sections were rinsed with HBS buffer and incubated with 0.0001 wt % DAPI and 10 μM of **1** in HBS for 10 min at room temperature. After being washed twice with ice-cooled 0.5 mM aqueous $Zn(NO_3)_2$, the tissue section was coated with aqueous mounting media (PermaFluor, Beckman Coulter) and subjected for fluorescence imaging through confocal laser scanning microscopy (FV-1000, Olympus) using an optimal excitation laser and detection wavelength window for each fluorescent dye (DAPI, λ_{ex} = 351 nm, λ_{em} = 400−500 nm; **1**, λ_{ex} = 488 nm, λ_{em} = 500−555 nm; AlexaFluor 633, λ_{ex} = 630 nm, λ_{em} = 645−745 nm). Several fluorescence images of the same tissue section were merged into one, using image processing software (Photoshop 6.0; Adobe Systems, Inc.).

Results and Discussion

Design and Synthesis of the BODIPY-Based Fluorescent Probe. Recently, we reported that the binuclear zinc complexes of 2,2′-dipicolylamine (Dpa) serve as artificial receptors for phosphorylated peptides.[14,15] For example, the bipyridyl-type Zn(II) complex **3** (Figure 1) binds to a bis-phosphorylated peptide with high affinity (K_d = ca. 0.1 μM) via a two-point metal−ligand interaction between the Zn(II)−Dpa sites and the pair of phosphate groups. The complex **3** is not applicable, however, to the fluorescence detection of hyperphosphorylated proteins because of its poor fluorescent properties, including a very weak emission (Φ < 0.1) and short excitation and emission wavelengths (<450 nm). To improve upon this performance, in this study we designed a new probe **1** for the efficient fluorescence detection of hyperphosphorylated tau protein. In the molecular design of **1**, we employed BODIPY as the fluorescent unit; it displays a bright fluorescence in the visible region (>500 nm). We connected the two Zn(II)−Dpa units directly to the BODIPY moiety (i.e., without using alkyl linkers) to provide the system with a rather planar and rigid conformation, which we suspected would provide stronger interactions with the β-sheet-rich structure of the NFTs. We introduced two triethylene glycol chains to impart the probe with sufficient solubility in aqueous solutions. Scheme 1 outlines our synthetic route toward **1**. Briefly, the acid-catalyzed condensation between the aldehyde **4** and 2,4-dimethylpyrrrole yielded **5**, which we treated with iodine and then complexed with boron trifluoride to give **7**. Compound **7** was converted to **9** via Suzuki coupling with the pyridyl pinacolylborane **8**; subsequent acid-catalyzed deprotection and reductive amination with 2-aminomethylpicoline gave the bis-Dpa ligand **11**. Finally, complexation with 2 equiv of $Zn(NO_3)_2$ yielded the probe **1**, which we characterized using ^{1}H NMR spectroscopy and elemental analysis. Details of the synthetic procedure of **1** are provided in the Supporting Information. As a control fluorescence probe, we also prepared the mononuclear Zn(II)−Dpa complex **2** using a synthetic route similar to that for **1** (Supporting Information).

Fluorescence Titration with Phosphorylated Tau Fragment Peptides. The absorption and emission maxima of probe **1** appear at 520 and 547 nm, respectively. For our purposes, the fluorescence quantum yield of **1** was sufficiently high (Φ = 0.31) under neutral aqueous conditions (50 mM HEPES, pH 7.2). Initially, we evaluated the sensing ability of **1** through fluorescence titration with a series of phosphorylated peptides (Table 1), all of which are fragment peptides derived from the hyper-phosphorylated human tau protein. Figure 2 displays a typical fluorescence change for the titration with the tau(227−238)-2P peptide, which possesses phospho-threonine and -serine residues at the (i, i+4) positions. The emission intensity of **1** increased by up to ca. 1.5-fold, with a typical saturation behavior, upon the gradual addition of tau(227−238)-2P peptide. Through curve-fitting analysis of the emission change, we estimated the dissociation constant (K_d) to be 7.5 μM. The fluorescence Job's plot indicated that the binding stoichiometry was 1:1 (Supporting Information). We obtained a similar value for the dissociation constant (K_d = 9.1 μM; n = 1.06; ΔH = 7.13 kcal/mol; $T\Delta S$ = 13.9 kcal/mol) when using isothermal titration calorimetry (ITC; see the Supporting Information), confirming that the emission response of **1** directly reflects its binding with the tau(227−238)-2P peptide. We observed no changes in fluorescence for mixtures of **1** with either the mono- or the nonphosphorylated tau(227−238)-1P and tau(227−238)-0P peptide (Figure 2b). The fluorescence of the mononuclear Zn(II) complex **2** did not change after the addition of bis-phosphorylated tau(227−238)-2P (data not shown). These results suggest that two-point binding, using both Zn(II)−Dpa sites of **1**, is essential for strong binding to and fluorescence sensing of bis-phosphorylated peptides. Table 1 reveals that **1** can also fluorescently sense the bis-phosphorylated tau(394−403)-2P and tau(204−217)-2 Pa and peptides and the tris-phosphorylated Tau(204−216)-3P peptide, all of which possess two-phosphorylated residues at (i, i+4) positions.

(14) (a) Ojida, A.; Hamachi, I. *Bull. Chem. Soc. Jpn.* **2006**, *79*, 35–46. (b) Ojida, A.; Inoue, M.; Mito-oka, Y.; Tsutsumi, H.; Sada, K.; Hamachi, I. *J. Am. Chem. Soc.* **2006**, *128*, 2052–2058. (c) Ojida, A.; Mito-oka, Y.; Sada, K.; Hamachi, I. *J. Am. Chem. Soc.* **2004**, *126*, 2454–2463. (d) Ojida, A.; Inoue, M.; Mito-Oka, Y.; Hamachi, I. *J. Am. Chem. Soc.* **2003**, *125*, 10184–10185.

(15) Grauer, A.; Riechers, A.; Ritter, S.; König, B. *Chem.-Eur. J.* **2008**, *14*, 8922.

Scheme 1. Synthesis of Probe **1**

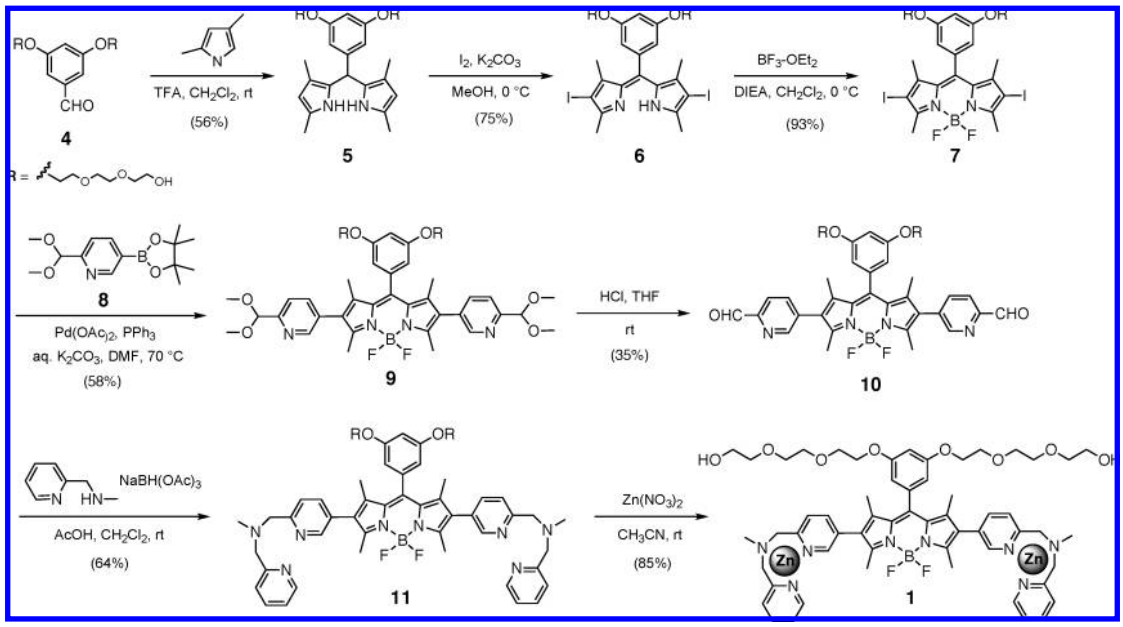

Table 1. Dissociation Constants (K_d) for the Binding of **1** to Tau Peptides[a]

peptide	sequence	positions of phosphorylated amino acid residues	K_d (μM)
tau(227-238)-2P	YAVVRpTPPKpSPSS	*i*, *i*+4	7.5
tau(394-403)-2P	YKpSPVVpSGDT	*i*, *i*+4	4.0
tau(204-217)-2Pa	YGTPGpSRSRpTPSLPT	*i*, *i*+4	40
tau(204-217)-3P	YGTPGpSRSRpTPpSLPT	*i*, *i*+4, *i*+6	4.3
tau(204-217)-2Pb	YGTPGpSRSRTPpSLPT	*i*, *i*+6	—[b]
tau(231-238)-2P	YTPPKpSPpSS	*i*, *i*+2	—[b]
tau(227-238)-1P	YAVVRTPPKpSPSS	—	—[b]
tau(227-238)-0P	YAVVRTPPKSPSS	—	—[b]

[a] Values of K_d were determined through analysis of fluorescence titration curves using nonlinear least-squares curve-fitting.[b] This value of K_d was not determined because only a small change in fluorescence intensity occurred after addition of the peptide.

On the other hand, no fluorescence change was induced by the tau(231−238)-2P and tau(204−217)-2Pb peptides, which possess their two phosphorylated residues at (*i*, *i*+2) and (*i*, *i*+6) positions, respectively. These results suggest that **1** binds preferably to bis-phosphorylated (*i*, *i*+4) peptides. We ascribe this sequence selectivity to the rigid structure of **1**, which results in rather strict distance-discrimination of the two phosphorylated residues in the peptides.

Selective Binding to in Vitro Aggregates of Hyperphosphorylated Tau Protein. Next, we evaluated the binding ability of **1** toward the in vitro aggregate of the phosphorylated tau protein (p-Tau). p-Tau was obtained through treatment of the recombinant full-length tau441 protein with GSK-3β (glycogen synthase kinse-3β), a representative protein kinase associated with the hyperphosphorylation event of tau protein.[3a] Quantitative in-gel fluorescence analysis revealed that each protein presented an average of 6.1 phosphorylation sites (see the Supporting Information for details). Using a literature method,[11] we performed the fibrillization of p-Tau through long-time incubation (>24 h) with heparin as an aggregation promoter; the morphology of the protein aggregate was confirmed through TEM analysis (Supporting Information). Figure 3a reveals a significant increase in the fluorescence of **1** after addition of the p-Tau aggregate in the nanomolar concentration range, suggesting that the binding affinity of **1** was greatly enhanced as compared to that for the phosphorylated peptide fragments (Table 1). From this fluorescence binding assay, we obtained a value of 9 nM for the EC_{50} of **1** toward the p-Tau aggregate (Figure 3b). We ascribe this affinity enhancement to a multivalent binding effect in the coordination of **1** with the multiple phosphorylation sites of p-Tau, as well as to the hydrophobic interactions between the planar BODIPY unit of **1** and the β-sheet-rich structure of the fibrils. This binding affinity is significantly stronger than that for the in vitro aggregate prepared from nonphosphorylated tau (n-Tau; EC_{50} = 80 nM), which we obtained using a similar procedure. These results clearly indicate that **1** exhibits phospho-selective binding behavior. Interestingly, we obtained a value of 650 nM for the EC_{50} of the peptide fibril composed of Aβ_{1-42} (Figure 3b), suggesting that the interaction of **1** with the Aβ_{1-42} fibril is much weaker by ca. 70-fold relative to that of the p-Tau protein aggregate. This finding is reasonable when considering the fact that

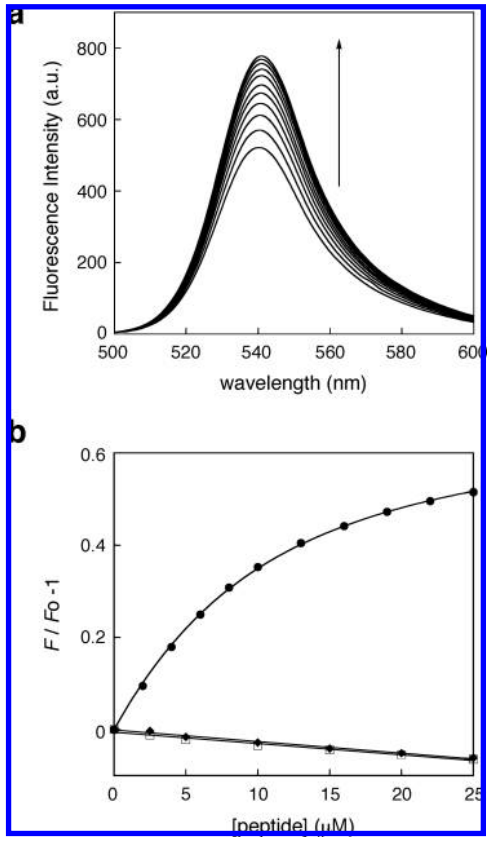

Figure 2. Fluorescence titration analysis for the binding of **1** with phosphorylated tau peptides. (a) Fluorescence spectral change of **1** (5 μM) upon addition of the bis-phosphorylated tau peptide, tau(227−238)-2P (0, 2, 4, 6, 8, 10, 13, 16, 19, 22, 25 μM). (b) Plot of the fluorescence intensity of **1** (λ_{em} = 545 nm) upon addition of the bis-phosphorylated tau(227−238)-2P (●), monophosphorylated tau(227−238)-1P (◆), and nonphosphorylated tau(227−238)-0P (□) peptides. Measurement conditions: 50 mM HEPES, pH 7.2, 25 °C.

multivalent coordination is unlikely to exist in the binding with the Aβ_{1-42} fibril. We used fluorescence microscopy to visualize the interactions of **1** with these aggregates (Figure 4). The fluorescence of **1** was clearly evident on the fibrous aggregates of p-Tau deposited on a glass slide (Figure 4e); it coincided well with the fluorescence image of the sample stained with thioflavin-T, a nonselective fluorescent probe for β-sheet structures of protein aggregates (Figure 4a).[16] Interestingly, the fluorescence image of **1** almost disappeared when we conducted the staining process in the presence of a high concentration of pyrophosphate anions (100 μM), a competitive binder for the Zn(II)−Dpa unit of **1** (Figure 4f).[17] In addition, neither the nonphosphorylated n-Tau nor Aβ_{1-42} aggregates exhibited fluorescence behavior when stained with **1** (Figure 4g and h, respectively). Thus, these fluorescence microscopy analyses further supported the notion of selective binding of **1** to the p-Tau aggregate; more importantly, they demonstrated the potential for using **1** to visualize NFTs in brain tissue with sufficient discrimination from SPs comprising aggregates of Aβ.

Histological Staining of NFTs in AD Brain Tissue. Next, we used **1** as a fluorescent staining agent for histological imaging of a hippocampus tissue section from the brain of an AD patient (Figure 5). Short-term incubation (10 min) of the tissue section

(16) Leliveld, S. R.; Korth, C. *Neurosci. Res.* **2007**, *85*, 2285–2297.
(17) Ojida, A.; Takashima, I.; Kohira, T.; Nonaka, H.; Hamachi, I. *J. Am. Chem. Soc.* **2008**, *130*, 12095–12101.

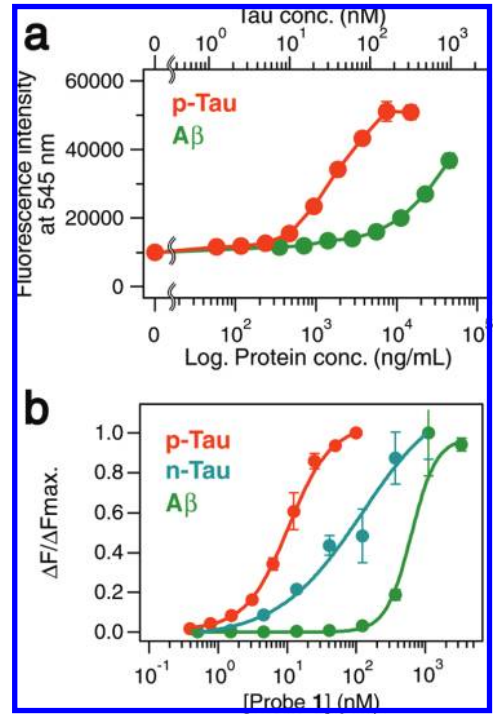

Figure 3. Fluorescence titration profiles of **1** with in vitro aggregates of p-Tau, n-Tau, and Aβ_{1-42}. (a) Changes in the fluorescence emission of **1** (100 nM) upon the addition of p-Tau (orange) and Aβ_{1-42} aggregate (green); error bars represent s.d. (b) Fluorescence binding assay for the interactions of **1** with the aggregates (1 μg/mL) of p-Tau (orange), n-Tau (blue), and Aβ_{1-42} (green); error bars represent s.d.

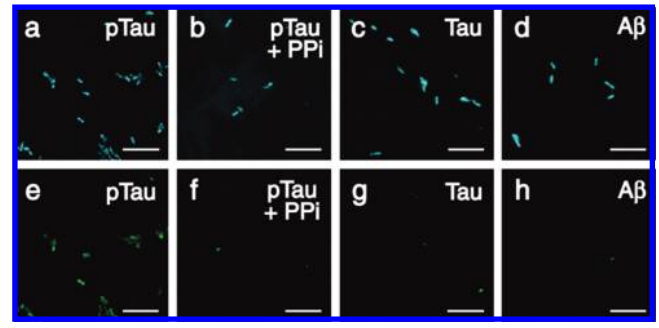

Figure 4. Fluorescence microscopy analyses of the in vitro aggregates of p-Tau, n-Tau, and Aβ_{1-42} stained with (a−d) thioflavin T and (e−h) **1**. In (b) and (f), the staining of p-Tau was conducted in the presence of sodium pyrophosphate (100 μM). Scale bars: 10 μm.

with **1** (10 μM) and subsequent washing with an aqueous solution of $Zn(NO_3)_2$ (0.5 mM) afforded a stained sample that exhibited many bright dots under fluorescence microscopy analysis (Figure 5a and d). Gratifyingly, these dots coincided with those in the immuno-staining image of NFTs obtained using AT8, a monoclonal antibody for p-Tau (Figure 5b and e). The fluorescence image of **1** also overlapped well with the tissue section image obtained through staining with Tau2, a phosphorylation-independent monoclonal antibody for the tau protein (Figure 5g−i). In contrast, fluorescent dots were scarce in the samples of the normal hippocampus tissue section that had been stained with **1** and AT8 (Figure 5p−r). These results strongly suggested that **1** can be used to fluorescently visualize NFTs deposited in the brain tissues of AD patients. The fluorescence image of **1** almost disappeared when we pretreated the brain tissue section with protein phosphatase 2A (PP2A),[13] although the deposited NFTs could still be detected after corresponding

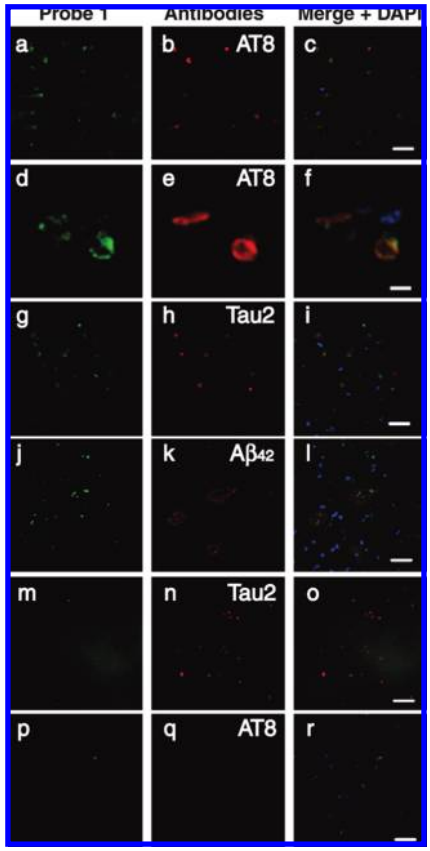

Figure 5. Fluorescence immunohistochemical analyses of hippocampus tissue sections from an AD patient. (a−c) Images of the tissue section triple-stained with **1**, AT8 (anti-p-Tau monoclonal antibody), and DAPI: (a) staining with of **1** (green); (b) staining with AT8 (red); (c) superimposition of images (a) and (b) and that obtained through staining with DAPI (blue). (d−f) Magnified images of (a−c). (g−i) Images of the tissue section triple-stained with **1**, Tau2 (phosphorylation-independent monoclonal antibody for tau), and DAPI: (g) staining with **1** (green); (h) staining with Tau2 (red); (i) superimposition of images (g) and (h) and that obtained through staining with DAPI (blue). (j−l) Images of the tissue section triple-stained with **1**, Aβ42 (anti-Aβ_{1-42} monoclonal antibody), and DAPI: (j) staining with **1** (green); (k) staining with Aβ42 (red); (l) superimposition of images (j) and (k) and that obtained through staining with DAPI (blue). (m−o) Images of the tissue section double-stained with **1** and Tau2 (phosphorylation-independent monoclonal antibody for tau) after dephosphorylation with PP2A: (m) staining with **1** (green); (n) staining with Tau2 (red); (o) superimposition of images (m) and (n). (p−r) Images of hippocampus tissue section from healthy adult, triple-stained with **1**, AT8, and DAPI: (p) staining with **1** (green); (q) staining with AT8 (red); (r) superimposition of images (p) and (q) and that obtained through staining with DAPI (blue). Scale bars: 50 μm (a−c, g−r); 10 μm (d−f).

treatment with the immuno-staining Tau2 antibody (Figure 5m−o). This result clearly indicates that coordination of **1** with the phosphate groups of p-Tau is crucial for the effective detection of NFTs, in good agreement with the results of our titration and staining experiments using the fibrous aggregates in vitro (Figures 3 and 4). Our most significant finding is that **1** can be used to visualize NFTs, but not SPs composed of Aβ, in the brain tissue section of an AD patient. Figure 5j−l reveals that the deposit pattern of the NFTs was distinct from that of the SPs; the NFTs detected by **1** are randomly distributed as small dots, whereas the SPs detected through immuno-staining with anti-Aβ antibody exist as larger (>50 μm) oval-shaped aggregates. Overall, these results indicate the applicability of using **1** for the selective detection of NFTs in brain tissue sections, with sharp discrimination from SPs; indeed, they demonstrate the validity of the molecular design of **1** as an NFT-specific probe that operates based on multivalent coordination.

Conclusion

We have prepared a new BODIPY-type zinc complex **1** that functions as a fluorescent probe that allows the imaging of NFTs, materials representative of many neurodegenerative disorders (including AD), in brain tissue samples. We exploited the phospho-selective binding properties of **1** to realize the selective detection of NFTs through the coordination of **1** with the multiple phosphate groups of the hyperphosphorylated tau protein. The probe **1** is the first example of a rationally designed small molecule that displays a high detection selectivity for NFTs over SPs; such selectivity is not readily achieved with other small molecular probes, which have been designed mainly to recognize the hydrophobic clefts of the β-sheet structure that commonly appears in these protein aggregates. From a histological staining experiment using brain tissue from an AD patient, **1** differentiated between the deposit patterns and localization sites of the NFTs and SPs. Thus, **1** appears to have great applicability for use in the precise and rapid detection of NFTs without the need for time-consuming immuno-staining with expensive antibodies. We believe that **1** will be an excellent tool for the precise pathological understanding and diagnosis of tau protein-related neurodegenerative disorders, including AD. Further applications of **1** and related derivatives for in vivo imaging studies are currently in progress.

Acknowledgment. This study was supported by the Innovative Techno-Hub for Integrated Medical Bioimaging Project of the Special Coordination Funds for Promoting Science and Technology, from the Ministry of Education, Culture, Sports, Science, and Technology (MEXT), Japan, and by the Sumitomo Foundation, Japan.

Supporting Information Available: Western blot analysis of synthetic tau protein; TEM analysis of p-Tau and n-Tau fibrils; procedures for the syntheses of **1** and **2**. This material is available free of charge via the Internet at http://pubs.acs.org.

JA9008369